Acta Oceanol. Sin., 2023, Vol. 42, No. 5, P. 79–92
https://doi.org/10.1007/s13131-022-2064-7
http://www.aosocean.com
E-mail: ocean2@hyxb.org.cn

Impacts of human activities on morphological evolution in the Modaomen Estuary, China

Tiehan Liao[1, 2], Haigang Zhan[1, 3*], Xing Wei[1, 3], Weikang Zhan[1, 3]

[1] State Key Laboratory of Tropical Oceanography, South China Sea Institute of Oceanology, Chinese Academy of Sciences, Guangzhou 510301, China

[2] University of Chinese Academy of Sciences, Beijing 100049, China

[3] Southern Marine Science and Engineering Guangdong Laboratory (Guangzhou), Guangzhou 511458, China

Received 22 November 2021; accepted 6 May 2022

Abstract

The morphology of the Modaomen Estuary (ME) has undergone drastic changes in recent decades, and quantifying the contribution of human activities and natural processes is crucial for estuary management. Using Landsat images, chart data, and hydrological and meteorological data, this study analyzed the evolution of the shoreline and subaqueous topography of the ME and attempted to quantify the extent of the contributions of human activities. The results show that local human activities dominated morphological evolution in some periods. From 1973 to 2003, the shoreline advanced rapidly seaward, resulting in approximately half of the water area being converted into land. Human activity is critical to this process, with the direct contribution of local land reclamation projects reaching more than 85%. After 2003, the shoreline remained relatively stable, probably due to a decrease in land reclamation projects. Regarding the evolution of subaqueous topography, the shoals in the estuary were heavily silted and gradually disappeared during 1983–2003, and the waterways narrowed and deepened. The average siltation rate decreased from 15.43 mm/a to –1.02 mm/a, indicating that the ME changed from sedimentation to slight erosion. By detecting variations of sediment load, we found that upstream human activities reduced river sediment, while downstream human activities significantly increased sediment input to the ME, leaving little change in the actual sediment input to the ME for a relatively long period. In addition, based on the empirical relationship between the sediment input and siltation rate, local human activities influenced the shift in the siltation state more than upstream and downstream human activities did. These findings suggest that more attention should be paid to local human activities to improve the estuarine management in the ME.

Key words: Modaomen Estuary, morphological evolution, human activity, quantitative analysis

Citation: Liao Tiehan, Zhan Haigang, Wei Xing, Zhan Weikang. 2023. Impacts of human activities on morphological evolution in the Modaomen Estuary, China. Acta Oceanologica Sinica, 42(5): 79–92, doi: 10.1007/s13131-022-2064-7

1 Introduction

In recent decades, many river deltas are experiencing serious problems due to the combined effects of human intervention and climate change (Day and Giosan, 2008). Due to the need for economic development, the morphological evolution and hydrodynamic system of rivers and estuaries are more disturbed by human activities than natural factors (Acciarri et al., 2016; Liu et al., 2014). For example, human activities including extensive land reclamation, channel deepening, sand mining, dam construction, and sea defense structure construction have important effects on the morphology of rivers and estuaries (Roccati et al., 2019; Wu et al., 2016a, 2016b; Yang et al., 2003, 2006; Zhang et al., 2015).

Among all kinds of human activities, land reclamation can visually and dramatically modify estuarine morphology (Healy and Hickey, 2002). However, as an influential potential factor in estuarine evolution, sediment supply changes, especially those caused by human activities upstream, are often underappreciated. In a typical case, the construction of dams may reduce river sediment load and alter the siltation state of estuaries (Dai et al., 2008). According to the latest Global Reservoir and Dam Database, 7 320 reservoirs and associated dams have been constructed on rivers worldwide, with a cumulative storage capacity of 6 863.5 km^3 (Lehner et al., 2011). After being extensively disturbed by human activities, especially dam and reservoir construction, 37% of rivers longer than 1 000 km remain free flowing over the entire river (Grill et al., 2019).

In this situation, many rivers experience sediment load reduction. With the completion of the Aswan High Dam, there was almost no net sediment input to the Nile Delta, although there was a sediment input of 100 Mt/a to 124 Mt/a before the construction of the dam (Fanos, 1995; Frihy et al., 2003; Stanley and Warne, 1993). The Changjiang River, the largest river in China, delivered approximately 490 Mt/a of sediment to the ocean in the 1950s and 1960s. However, the sediment load was reduced to 150 Mt/a after completion of the Three Gorges Dam (Yang et al., 2011). Sediment reduction dominates the transition from net ac-

Foundation item: The National Natural Science Foundation of China under contract Nos 41876205, 42106169 and 41890851; the Key Special Project for Introduced Talents Team of Southern Marine Science and Engineering Guangdong Laboratory (Guangzhou) under contract Nos GML2019ZD0305 and GML2019ZD0303; the Project of State Key Laboratory of Tropical Oceanography under contract Nos LTOZZ2102 and LTOZZ2202.

*Corresponding author, E-mail: hgzhan@scsio.ac.cn

cretion to erosion in some reaches of the Changjiang River and the change from accretion to recession along the estuary (Dai and Liu, 2013; Dai and Lu, 2014; Luo et al., 2012; Yang et al., 2007, 2011). Studies have shown that after the Three Gorges intercepted a large amount of sediment, some large lakes and the riverbed of the middle-lower Changjiang River became the main sources of sediment and played a critical role in the evolution of the Changjiang River depositional system (Dai et al., 2018). Landward sediment transport from the coastal area is also an influential factor in maintaining the current sedimentation state of the Changjiang River Estuary, and tropical cyclones seem to enhance sediment transport (Dai et al., 2018; Dai, 2021; Wang et al., 2020).

In the past few decades, along with economic development, the Zhujiang River Delta has also been affected by many anthropogenic disturbances, such as the upstream construction of reservoirs, sand mining in the river, coastal land reclamation, deepening of shipping channels, and building of breakwaters. With various human activities constantly altering the hydrological environment, the Zhujiang River ranks among the most regulated rivers on Earth (Nilsson et al., 2005). Because of the prominent effects of human intervention on hydrological processes, scholars have begun to assess the relationship between human activities and the temporal and spatial variations in runoff and sediment load in the Zhujiang River (Chen et al., 2011; Dai et al., 2008; Liu et al., 2014; Zhang et al., 2009; Zhang and Lu, 2009). Moreover, studies have been conducted on the link between morphological changes and human intervention based on nautical charts (Chu et al., 2013; Wei et al., 2021; Wu et al., 2016a, 2016b, 2018; Zhang et al., 2015). However, due to the complex interactions between human activities and estuarine morphology evolution, most studies have only discussed the effects of human activities on estuarine morphology qualitatively and rarely involved quantitative analysis. Quantifying the impact of human activity on estuarine evolution would greatly improve estuarine development management. Mei et al. (2015) successfully assessed the contributions of climate change, human activities, and the Three Gorges Dam regulation to the dramatic recession of Poyang Lake by using multiple data. This work provides a reference of our attempts to quantify human impacts on the evolution of the Modaomen Estuary (ME).

The ME area is one of the most notable regions in the Zhujiang River Delta for economic development. With the establishment of the Guangdong-Hong Kong-Macao Greater Bay Area, the locational advantage of the ME is increasingly prominent. In this case, human intervention may be involved in estuary management. There is an urgent need to understand the relationship between human activity and the evolution of estuarine morphology. By analyzing Landsat images, chart data, and hydrological and meteorological data, we aimed to (1) characterize the evolution of the shoreline and subaqueous topography, (2) explore and quantify the contribution of the influence of human activities on the shoreline change and the local siltation state transition.

2 Materials and methods

2.1 *Study area*

The Zhujiang River has a complex river network system and three main tributaries (the Xijiang River, Beijiang River, and Dongjiang River). Among the three tributaries, the Xijiang River delivers the highest runoff and sediment load in the Zhujiang River Delta. Our study area, the ME, is the main outlet of the Xijiang River. The detailed study area is illustrated in Fig. 1, which

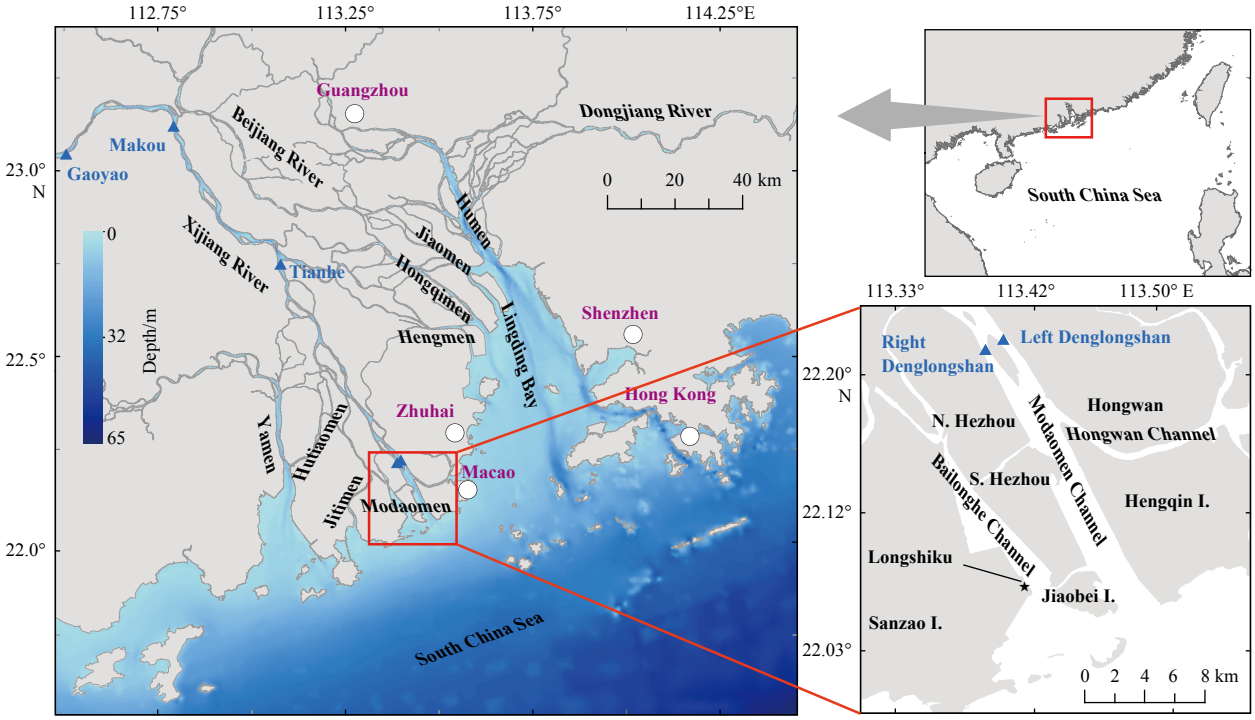

Fig. 1. Geographical location of the study area. The Zhujiang River Delta (ZRD) comprises the marked study area and the study region with detailed geographic information. The three major tributaries of the Zhujiang River (Dongjiang River, Beijiang River, and Xijiang River) and eight main outlets (Humen, Jiaomen, Hongqimen, Hengmen, Modaomen, Jitimen, Hutiaomen, and Yamen) are shown. The major cities in the ZRD are marked. Blue triangles represent the Makou, Gaoyao, Tianhe, Left Denglongshan, and Right Denglongshan hydrological stations. The bottom right panel exhibits the geographic information of Modaomen Estuary where this study is focused. N.: North; S.: South; I.: Island.

extends from 21°59′43″N to 22°14′31″N, and 113°18′44″E to 113°32′46″E.

ME is the foremost outlet for river runoff and sediment transportation among the eight main outlets of the Zhujiang River. When transported into the South China Sea via the ME, the average fluvial discharge flux was up to 88×10^9 m^3/a, approximately 28% of the total runoff load of the Zhujiang River. In addition, 23 Mt/a of sediment entered the ME on average. This amount is one-third of the total sediment load transported by the Zhujiang River. For the four west outlets, the ME accounts for approximately 74% and 77% of river runoff and sediment transportation, respectively. Most of the sediment load and fluvial discharge supplied to the ME is measured at the Makou. Regarding tidal dynamics, the mean tidal range in the ME is 0.86–1.11 m, and the flood duration is shorter than the ebb duration (Gong and Shen, 2011). Weak tidal dynamics may favor the sedimentation of the ME.

2.2 *Data collection and processing*

In the following discussion sections, monthly runoff data and sediment data observed at the Makou hydrological station (Fig. 1), precipitation and soil erosion data in the Zhujiang River Basin, and capacity data of the main reservoirs in the upper reaches of the Xijiang River are cited. Hydrological data were extracted from the *Bulletins of Chinese River Sediments* compiled by the Ministry of Water Resources of China (http://www.mwr.gov.cn/). Precipitation data were obtained from the National Meteorological Information Center (http://data.cma.cn/). Soil erosion data and reservoir-related statistics were extracted from the literature (Dai et al., 2008; Liu et al., 2018). In addition, sediment flux data from the main cross-sections of the Xijiang River were used to analyze the relationship between the sediment load at Makou and the ME. These data were obtained from the Zhujiang River Water Resources Commission of the Ministry of Water Resources (http://www.pearlwater.gov.cn/) for July 1999 (wet season) and February 2001 (dry season).

Because of the limited number of Landsat images, most of which were disturbed by clouds, obtaining many valuable images was difficult. We selected a clear image of a certain year. A series of Landsat images were collected from the United States Geological Survey (USGS; https://glovis.usgs.gov/app) to extract historical shorelines. The acquisition time of images ranged from 1987 to 2017 with an interval of 2 years, except for an individual image in 1973. The pixel resolution of the Landsat 5–8 images was 30 m, and 60 m for the Landsat 1 MSS sensor. Detailed information is provided in Table 1. All Landsat images were geometrically corrected using the Landsat product generation system code developed by the USGS (Loveland and Dwyer, 2012).

In this study, we used the normalized difference water index (NDWI) to distinguish between water and non-water pixels (McFeeters, 1996). Using the NDWI method, we could easily extract shorelines from remote sensing images. However, not all remote sensing images were captured in the same tidal state. If the coast is not steep, shorelines acquired at different tidal states may not be consistent. Correction methods are required to obtain the shorelines under the same tidal conditions. Shoreline digitization methods of manual intervention have proven to be successful and accurate (Kong et al., 2015; Matin and Hasan, 2021; Zhang et al., 2015). In this case, we used the NDWI method to derive the shoreline automatically and then obtained the shoreline at a mean high tide state with manual correction to the shoreline. Manual correction is based on shortwave infrared band and pseudocolor images.

Table 1. Basic information of used Landsat images

Acquisition time	Satellite	Sensor	Pixel resolution/m	Datum/ Ellipsoid	UTM zone
1973/12/25	Landsat 1	MSS	60	WGS84	49
1987/2/7	Landsat 5	TM	30	WGS84	49
1989/7/6	Landsat 5	TM	30	WGS84	49
1991/11/17	Landsat 5	TM	30	WGS84	49
1993/12/24	Landsat 5	TM	30	WGS84	49
1995/12/30	Landsat 5	TM	30	WGS84	49
1997/11/1	Landsat 5	TM	30	WGS84	49
1999/11/15	Landsat 7	ETM+	30	WGS84	49
2001/11/20	Landsat 7	ETM+	30	WGS84	49
2003/10/17	Landsat 5	TM	30	WGS84	49
2005/11/23	Landsat 5	TM	30	WGS84	49
2007/9/18	Landsat 7	ETM+	30	WGS84	49
2009/1/2	Landsat 5	TM	30	WGS84	49
2011/6/1	Landsat 5	TM	30	WGS84	49
2013/11/29	Landsat 8	OLI/TIRS	30	WGS84	49
2015/1/3	Landsat 8	OLI/TIRS	30	WGS84	49
2017/1/8	Landsat 8	OLI/TIRS	30	WGS84	49

To explore the evolution of the subaqueous topography of the ME, we collected nautical charts and underwater topographic survey data from 1964, 1983, and 2003 (Table 2). The bathymetric data in each chart were measured at the same time. The paper-based bathymetric data were then digitized using GIS software. Because the scattered bathymetric data were recorded based on the Theoretical Lowest Tide Surface, which was a datum associated with the mean sea level and varied by region. Through the relationship between the zero level of tide gauge and the Zhujiang River Datum, and the mean sea level calculated from the tide records, we got the transformation relation between the Theoretical Lowest Tide Surface and the Zhujiang River Datum. Then, using the datum transformation relations of several tide gauge stations during the bathymetry surveyed period, we could convert the chart bathymetry to the water depth relative to the Zhujiang River Datum. All bathymetric data were converted to the Zhujiang River Datum for an accurate comparison. Converting all bathymetric data to a uniform elevation datum also avoided the effect of sea-level changes on variations in bathymetric data. Thereafter, the kriging interpolation method was used to interpolate the scattered bathymetric data into a 20 m× 20 m grid. Finally, the bathymetric grid data were transformed into a digital elevation model (DEM). Using DEMs, comparing and analyzing the evolution of the subaqueous topography of the ME is possible.

Table 2. Topographic data

Map title	Projection coordinate	Depth datum	Scale	Measurement time
Sanzao Island and Related Sites	Beijing 54 Coordinate System	Theoretical Lowest Tide Surface	1:50 000	1964
Modaomen Channel Series	Beijing 54 Coordinate System	Theoretical Lowest Tide Surface	1:10 000	1983
Topographic Maps of Flood Control and Regulating Engineering in Zhujiang River Estuary	Beijing 54 Coordinate System	Theoretical Lowest Tide Surface	1:5 000	2003

2.3 *Calculation of shoreline change rate*

Various versions of the Digital Shoreline Analysis System (DSAS) are commonly used calculation tools for shoreline change-related analyses (Himmelstoss et al., 2018; Thieler et al., 2009). The DSAS performs well in coastal and island locations with open shorelines that are not complex (Cunliffe et al., 2019; Ford, 2013; Jones et al., 2011; Matin and Hasan, 2021). However, evaluating the continuous shoreline changes in complex estuarine shorelines is not convenient. In this study, we employed a point-based shoreline change detection method to obtain shoreline change information (Cowart et al., 2010).

For a certain temporal interval, this method requests the shoreline at the beginning of that period (old shoreline) and the shoreline at the ending of the period (new shoreline). The new shoreline is represented as a series of equally spaced points based on a spatial interval. An interval of 100 m was used in the study. Next, the shoreline change rate (SCR) was calculated by computing the shortest distance from the point on the new shoreline to the old shoreline. The position of the new shoreline relative to the old shoreline implies shoreline advancement or erosion, as indicated by $d_{\min}$.

SCR for a certain point on the new shoreline is calculated as follows:

$$\mathrm{SCR} = \frac{d_{\min}}{\Delta t}, \tag{1}$$

where $d_{\min}$ is the minimum distance from the point to the old shoreline for a certain time duration, and Δt is the time duration. A diagram of the point-based algorithm is shown in Fig. 2.

3 Results

An estuary is a partially enclosed coastal body of brackish water that is a region of transition from the river to the ocean (Pritchard, 1967). In this section, we analyze the morphological evolution of the ME from two aspects: shoreline change and underwater topography evolution. Research on shoreline change is mainly based on shoreline data extracted from 17 remote sensing images from 1972 to 2017. Underwater topography evolution trend analysis was based on estuarine bathymetric data from 1964, 1983, and 2003.

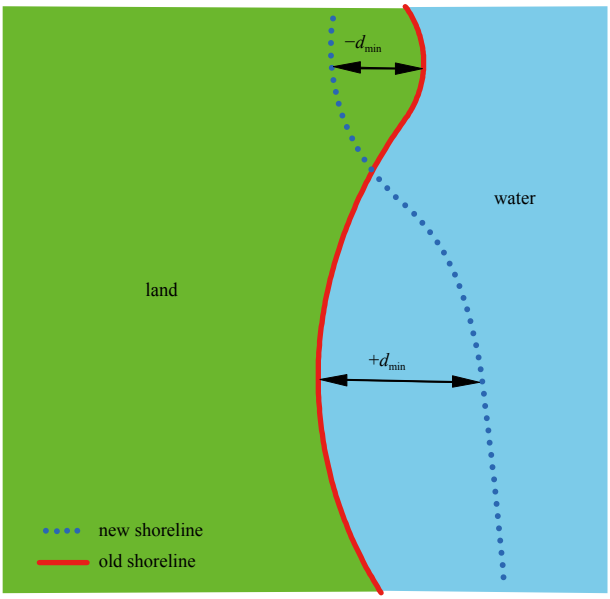

Fig. 2. Parameter definition of the point-based algorithm for calculating shoreline change rate. $d_{\min}$ indicates the minimum distance between the point on the new shoreline and the old shoreline.

3.1 *Shoreline evolution of the ME*

Shoreline analysis revealed the evolutionary trend of the ME. The most significant evolutionary trend was the transformation of water to land. As shown in Fig. 3a, the shoreline of the ME underwent dramatic changes. The shoreline advanced significantly from 1973 to 2017. In 1973, four major outfalls communicated the inner and outer water, namely, the northwestern outfall of Sanzao Island, the Longshiku, the Modaomen Channel, and the Hongwan Channel (Fig. 1). However, only the Modaomen and Hongwan channels remained free flowing in 2017. Although Longshiku was not transformed into land, it was no longer the main outlet for fluvial discharge and was only a tidal channel. Furthermore, the water outfall, located on northwestern Sanzao Island, had completely turned into land.

To accurately assess and compare shoreline variations, we had to divide the research period into small intervals. Limited by the time span and number of available remote sensing images, a fixed time interval may cause shoreline evolution to be exaggerated or reduced. Hence, we divided 1973–2017 into five periods based on the time when the shoreline experienced dramatic changes in 1973–1987, 1987–1991, 1991–1999, 1999–2003, and 2003–2017. The statistical calculations of shoreline changes were based on these five periods.

Shoreline changes usually lead to variations in water area. The water area and mean water area change rate (WACR) of the ME were calculated for each period, and the detailed results are shown in Fig. 3. From 1973 to 2003, the water area decreased from 368.78 km^2 to 188.24 km^2, a loss of 48.96%. Almost half of the water area was lost after 2003. By contrast, the water area decreased 0.37% between 2003 and 2017. Overall, the water area experienced rapid loss with a mean WACR of –6.02 km^2/a in 1973–2003. Among the five periods, the most marked change was in 1999–2003, with a mean WACR of –7.84 km^2/a. During the last period, the mean WACR was –0.05 km^2/a, indicating that the coastline remained relatively stable.

The mean SCR and WACR maintained almost synchronous changes among the periods (Table 3). A large mean WACR tended to correspond to a large mean SCR. In 2003–2017, shorelines were relatively stable, with a mean SCR of 1.06 m/a, an order of magnitude smaller than those in the other periods. The mean WACR in 1991–1999 was twice as large as that in 1987–1991, and the mean SCR in the former period was only 5% larger than that in the latter. Because SCRs were calculated based on a fixed shoreline distance, a considerable sticking out of the new shoreline would cause substantial variation in mean SCR to mismatch with the mean WACR change. Thus, the sharp stretch of the shoreline in 1999 on northwestern Hengqin Island (Fig. 4c) caused a mismatch in the magnitude of change between the mean SCR and mean WACR.

We reviewed the detailed SCRs in Fig. 4 and pronounced that the shoreline advanced almost in all coastal areas during the five periods, yet the rates differed among regions. In the first four periods, approximately 10% of the SCRs were greater than 100 m/a, with contributions of 60%–90% to the cumulative SCR. SCRs with large values were significant for the overall evaluation of shoreline evolution in the ME.

Large SCRs tended to exist in the patches, and these areas represented the most dramatic shoreline evolution during each

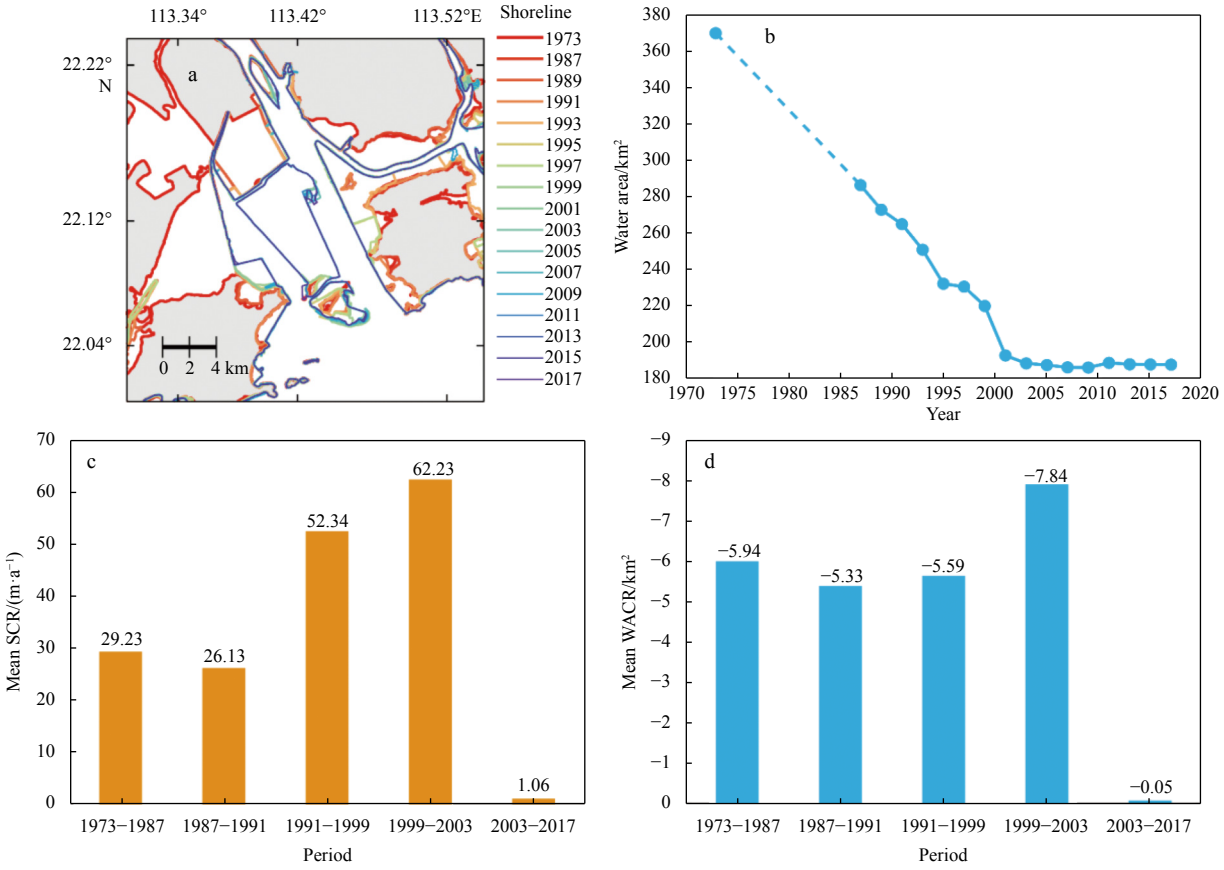

Fig. 3. Historical shoreline position (a), water area with study region in each year (b), mean shoreline change rate (SCR) in five intervals (c), and surface mean water area change rates in five intervals (d). WACR: water area change rate.

Table 3. Basic statistics of digital elevation model

	Survey time		
	1964	1983	2003
Area of water/km²	348.58	332.50	185.00
Volume of water/(10^6 m³)	931.98	782.67	620.25
Mean depth/m	2.67	2.35	3.35
Mean depth* /m	3.62	3.33	3.35

Note: *Mean depths were calculated within the water area in 2003.

period. Zones with severe shoreline changes during each period are marked as I –VII (Fig. 4). The shoreline evolution in each of these zones had a profound impact on the land–water pattern and the hydrodynamic environment of the ME. Zone III had a maximum SCR of 250 m/a. Shoreline changes in this area resulted in a decrease in shallows within the ME, as well as the disappearance of an essential tidal channel located on northwestern Sanzao Island. In Zone V, with a maximum SCR of 678 m/a, the extension of the shoreline narrowed the Hongwan Channel and weakened its hydrodynamic function. During 1999–2003, the maximum SCR in Zone VI was over 1 000 m/a, which was the largest among all periods. The water in the ME was further reduced, the tidal channel was further narrowed, and Zone VI was transformed into land from water. Most of the new shorelines in these zones were unnaturally smooth and straight in of morphology, with signs of human intervention.

From 1973 to 2003, the shoreline of the ME evolved dramatically, with almost half of the water area turning into land. Subsequently, the shoreline remained relatively stable. Detailed SCR analysis revealed that areas with the most dramatic shoreline changes existed in patches and appeared to show signs of human interference.

3.2 *Subaqueous topography evolution of the ME*

We constructed DEMs for the subaqueous topography in 1964, 1983, and 2003 on the basis of bathymetric data from nautical charts (Fig. 5). A historical analysis based on DEMs revealed remarkable modifications in the water area and underwater topography. As shown in Table 3, in 1964–1983, the water area decreased by 4.61%, and the volume of water below the datum decreased by 16.02%. In addition, the average depth decreased from 2.67 m to 2.35 m, a decrease of 11.96%. The geometry of the estuary experienced drastic variations from 1983 to 2003. During this period, the water area decreased from 332.5 km² to 185 km² in 2003, a decrease of 44.36%. The water volume decreased by 20.75%. By contrast, the mean water depth increased from 2.35 m in 1983 to 3.35 m. During 1964–1983, the ME experienced a general process of siltation and shallowing, whereas it experienced a process of erosion and deepening in 1983–2003.

Figure 6 shows the WACR at different depths during the three periods. This parameter visualizes the variations in the water area at different depths during the evolution of subaqueous topography. Large WACRs for all three periods were detected in the depth range of 0–2 m. Owing to enhanced shoal sedimentation from 1964 to 1983, the maximum WACR was observed at a depth of 1 m. However, the largest WACR was detected at a depth of 0 m for the time interval of 1983–2003, suggesting that water turning to land was a critical morphological process. Furthermore, the results showed a decrease (negative WACR) in the water area 4–

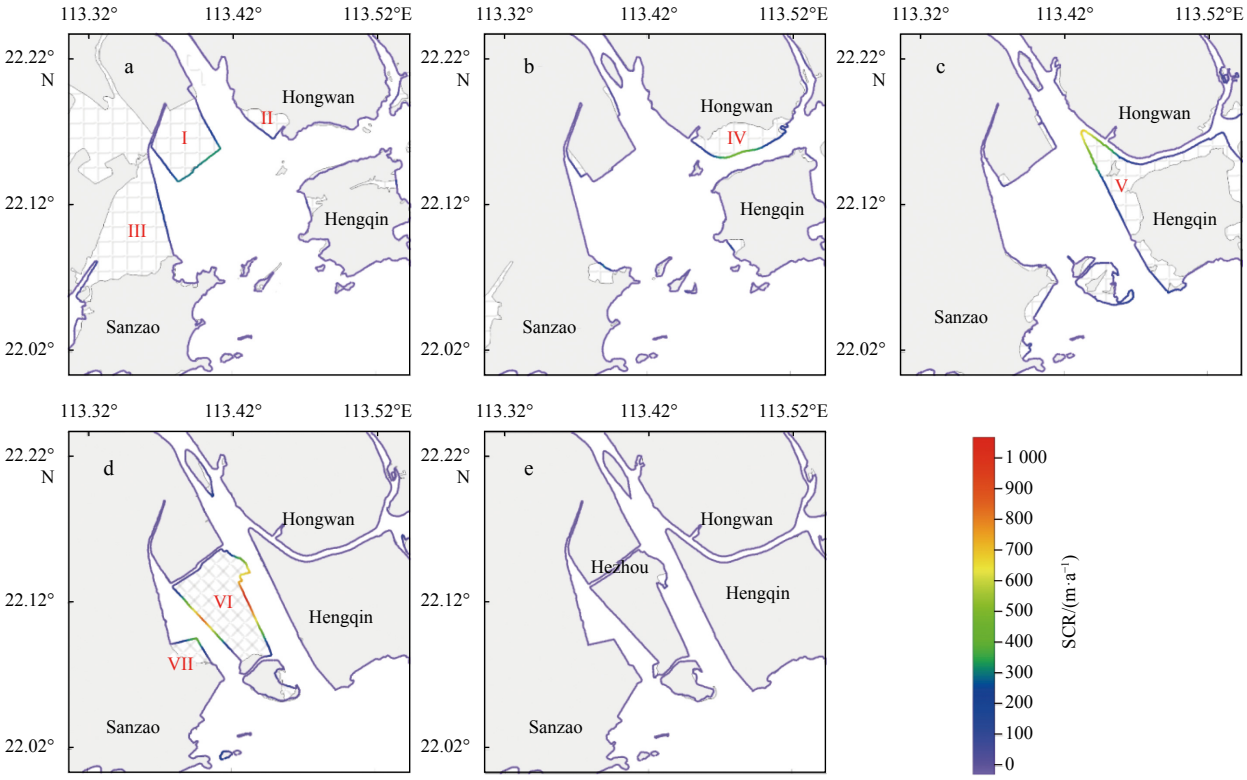

Fig. 4. Spatial distribution of shoreline change rate (SCR) in the Modaomen Estuary during the five divided periods. From a to e, the panels denote 1973–1987, 1987–1991, 1991–1999, 1999–2003, and 2003–2017, respectively.

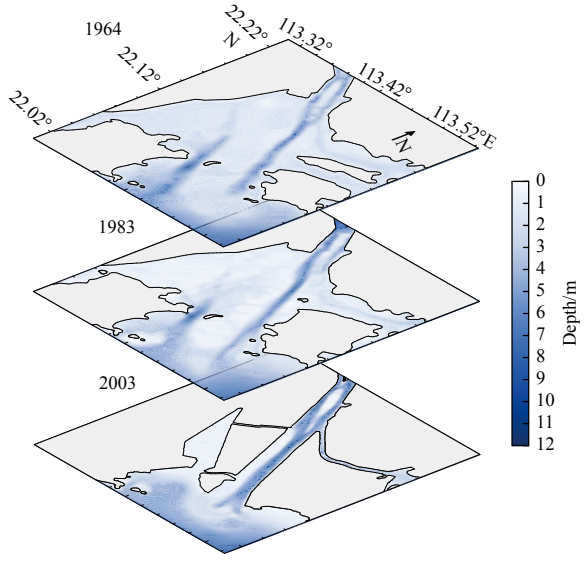

Fig. 5. Underwater topography of the Modaomen Estuary in 1964, 1983, and 2003.

5 m below the datum level during 1964–1983, and the water area increased (positive WACR) in the depth range of 4–8 m in 1983–2003. These findings indicate that the morphological evolutionary state varied between the two periods. Siltation was the dominant process during the former period. In the later period, there was a significant decrease in the surface water area, accompanied by an increase in the area among the intermediate depths. The statistics for the full span (1964–2003) were approximately equal to the average of the other two periods.

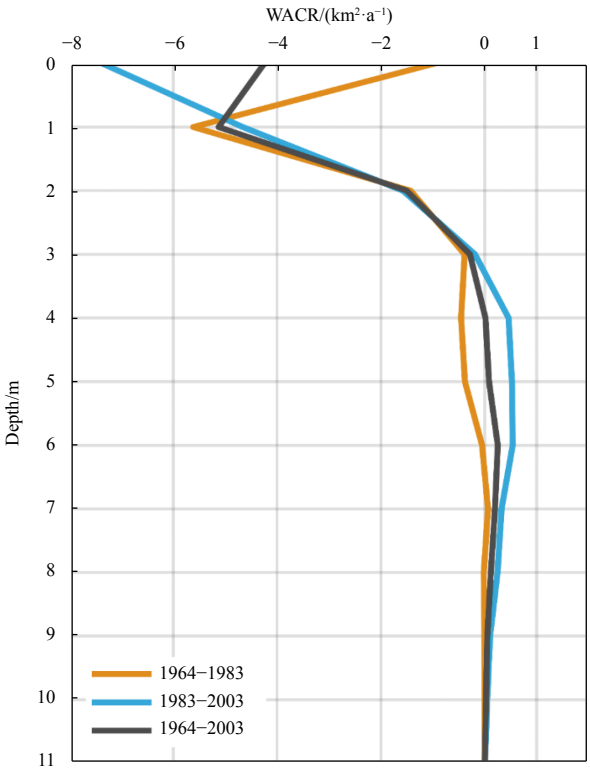

Fig. 6. Water area change rate (WACR) at different depths for three periods: 1964–1983, 1983–2003, 1964–2003.

As shown in Figs 5 and 7, from 1964 to 2003, the Modaomen and Hongwan channels were increasingly eroded and deepened,

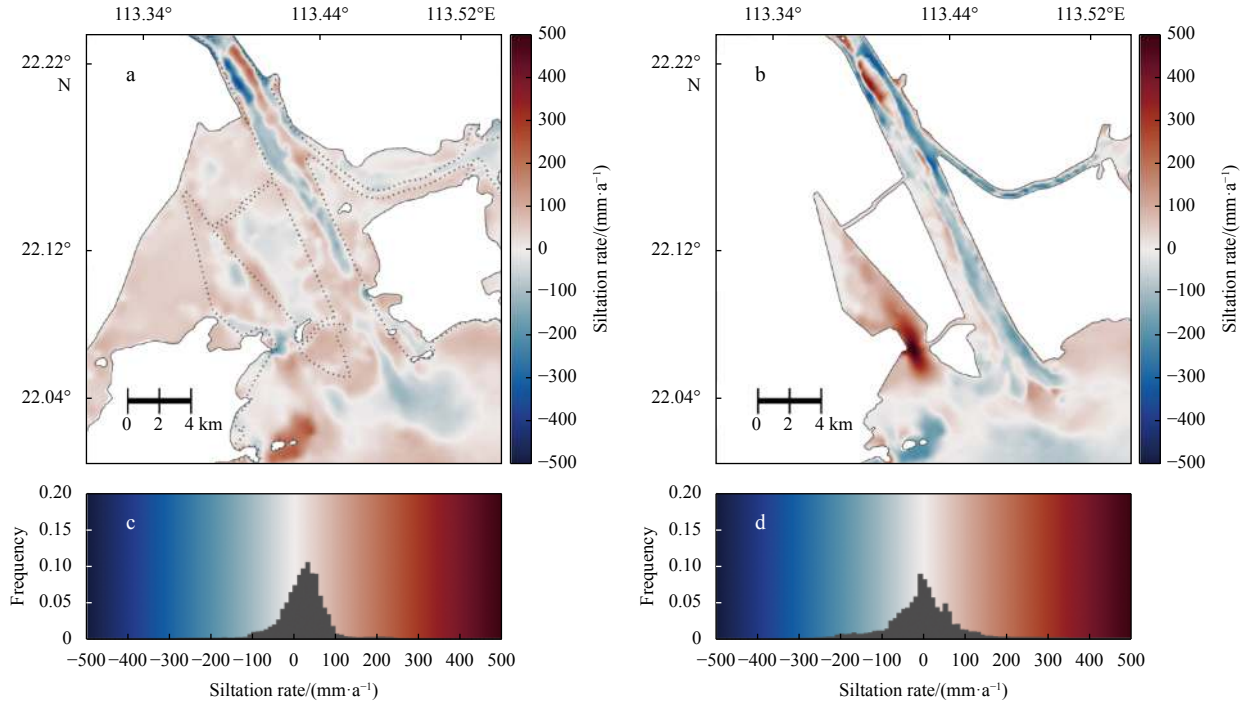

Fig. 7. Spatial distribution and corresponding frequency distribution of siltation rates in the Modaomen Estuary for 1964–1983 (a, c) and 1983–2003 (b, d). Dotted lines in a are the shorelines in 2003.

and most of the shallows in the west were shallowing. In 1964, the average water depth in the western shallows was approximately 4 m. Additionally, the deepest area in the west, Longshiku, was approximately 11 m deep. By 1983, only the Bailonghe Channel within the western shallows had greater depth. Due to no sufficiently deep channels to communicate with the main channel of the Xijiang River, the function of the Bailonghe Channel as a drainage path for runoff was reduced.

From 1964 to 2003, the area of siltation decreased as the eroded area increased (Table 4), whereas the overall mean siltation state changed from sedimentation in the early stages to slight erosion in the later stages. From 1964 to 1983, more than 70% of the underwater topography experienced increasing shallowing, and some portions of the Modaomen Channel increased in depth. From the histogram of frequency statistics on siltation rates (lower panels in Fig. 7) and Table 4, the net siltation of the ME during this period was 54.22×10^6 m^3 with an average positive siltation rate of 15.43 mm/a, showing a typical sedimentation state. During 1983–2003, many shallows in the west disappeared, and the remaining part became much shallower. By contrast, the Modaomen and Hongwan channels showed strong deepening characteristics. As shown in Table 4, the net siltation during this period decreased to -3.78×10^6 m^3, with an average siltation rate of –1.02 mm/a. The average siltation rate decreased by 107% compared with the rate in former period, and the underwater topography as a whole showed slight erosion, which markedly differed from the prior topography. Because the mean siltation rate represented the overall evolution trend of the subaqueous topography in the study area, we used it as a parameter for evaluating underwater topography evolution, and the mean siltation rate was related to anthropogenic factors for interpreting the subaqueous topography evolution mechanism.

4 Discussion

The evolution of estuarine morphology is a complex, dynamic process. Accurately evaluating natural processes and human activities is difficult. Human activities in estuaries are varied, namely, sand excavation, reclamation, channel dredging, and

Table 4. Statistics of siltation characteristics in each period

	Period		
	1964–1983	1964–1983*	1983–2003
Siltation amount (SA)/(10^6 m^3)	194.49	111.31	109.19
Erosion amount (EA)/(10^6 m^3)	73.99	57.09	112.97
Net siltation amount (NSA=SA–EA)/(10^6 m^3)	120.50	54.22	–3.78
Siltation area (SiA)/km^2	235.75	121.77	89.01
Erosion area (ErA)/km^2	96.75	63.23	95.99
Total research area (TRA=SiA+ErA)/km^2	332.50	185.00	185.00
Percentage of siltation area (SiA/TRA)/%	70.90	65.82	48.11
Percentage of erosion area (ErA/TRA)/%	29.10	34.18	51.89
Mean siltation rate (NSA/TRA/length of the period)/(mm·a^{-1})	19.07	15.43	–1.02

Note: *Parameters for this period were calculated within the water area in 2003.

embankment construction. Accurate assessments of the contribution of each type of human activity require a large amount of fine data. However, we had no means to access this data. In addition to the direct physical changes that human activity makes to estuaries, it has long-term effects on estuarine dynamics, further increasing the difficulty of separating the contribution of human activity from overall changes. Therefore, as a preliminary attempt to quantify the contribution of human activities to the morphological evolution of the ME, we used easily quantifiable reclamation data to demonstrate that human activities have dominated the evolution of shorelines in the ME. We did not conduct a detailed assessment of human activities.

To evaluate the impact of human activities on the submerged topography of the ME, we divided the Xijiang River into upstream reaches (reaches upstream Makou), downstream reaches (reaches between Makou and the ME), and the local region (the ME). The effects of upstream and downstream human activities on the ME were translated into variations in sediment input to the ME. We used a simple model of sediment input and the average sedimentation rate in the estuary to separate the contributions of human activities in the regions. Contributions of detailed human activities within each region were not assessed in this study.

4.1 *Upstream and downstream human activities altered river sediment transport*

Because river sediment input from the upper reaches is critical to the evolution of estuarine subaqueous topography, we first had to estimate whether sediment input was disturbed by anthropogenic influence. Before 1997, there was a relatively stable linear relationship between runoff and sediment transport (Fig. 8b). After 1997, the data points gradually deviated from the fitting line, implying that something occurred and reduced the observed sediment concentration at Makou. The decrease of sediment concentration may have resulted from reduced sediment production or a sediment decrease during transportation. River sediments mainly originate from soil erosion caused by precipitation (Gellis and Noe, 2013; Meade, 1982). As shown in Fig. 8d, the soil erosion area in the Zhujiang River Basin did not decrease after 1997. A Mann-Kendall Tau trend test was performed on the precipitation data, and we obtained a p value of 0.52, which indicates no significant trend in precipitation. A good correlation between runoff and precipitation indicated that the conversion rate from precipitation to river runoff remained essentially the same (Fig. 8a).

As shown in Fig. 8d, the soil erosion area did not decrease

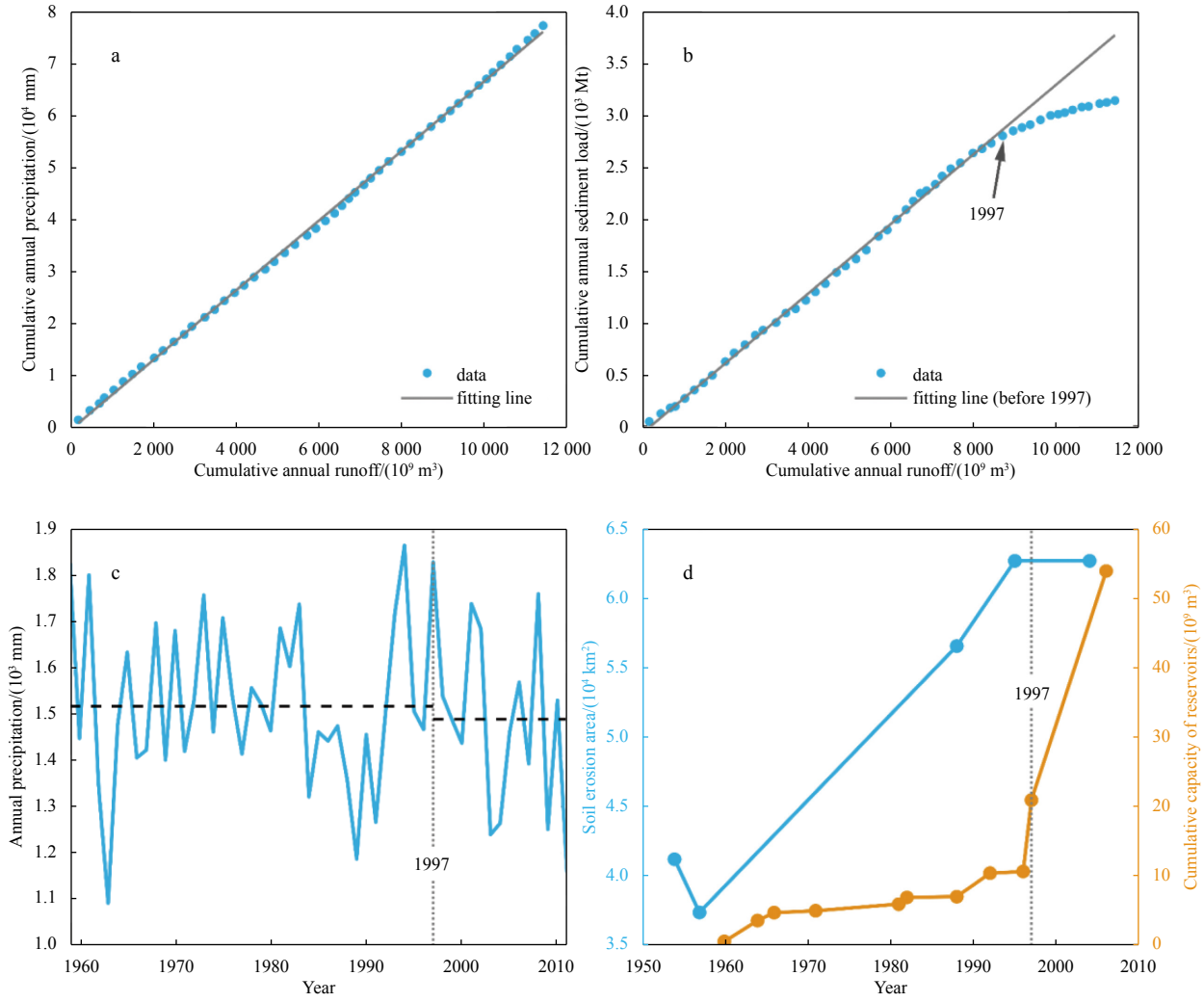

Fig. 8. Double mass curve in cumulative values of annual runoff and annual precipitation from 1960 to 2010 (a); double mass curve in cumulative values of annual runoff and annual sediment load for 1960–2010 (b); annual precipitation from 1959 to 2011 (c); area of soil eroded land and total storage capacity of reservoirs (d).

after 1997 and was even larger than before. Unreduced precipitation flows through the larger areas of soil erosion than before and is converted into river runoff with the same efficiency. Therefore, we inferred that river sediment production should not decline significantly. The decrease of river sediment after 1997 did not result from a decrease of sediment production but from sediment decreases during transportation.

According to historical data, there were no significant changes in the natural environment in the Zhujiang River Basin, which could have caused a significant decrease in sediment during transportation after 1997. Therefore, there is a high probability that sediment variation is caused by human activity. Among many human activities, river damming can trap large amounts of river sediment. In addition, river sand excavation for construction materials also decreases river sediment. The cumulative reservoir capacity in the upper Xijiang River (Fig. 8d) showed a dramatic increase in 1997, matching the shifting time in sediment concentration. Consequently, we inferred that human activity is a critical factor that decreases river sediment.

By applying the runoff–sediment relationship before 1997 to the data after 1997, we obtained the amount of sediment reduction due to human activities. We obtained a linear relationship between the logarithmic monthly runoff and sediment observed at Makou (Fig. 9). Based on the runoff–sediment relationship, we obtained the sediment flux without human interferences during 1997–2003. During 1997–2003, the estimated mean sediment flux was 76.38 Mt/a; the observed mean sediment flux was 44.34 Mt/a. The observed sediment was 58% of the estimated sediment; thus, human activities implemented in the upper reaches of the Xijiang River have a significant influence on river sediment transport. Studies in other large deltas have also revealed that upstream human activities (especially damming) have a significant impact on estuarine sediment input. After the completion of the Aswan High Dam, there was almost no net sediment input to the Nile Delta (Frihy et al., 2003; Stanley and Warne, 1993). Due to the completion of the Three Gorges Dam, the sediment input of the Changjiang River Delta was reduced about 70% (Yang et al., 2011).

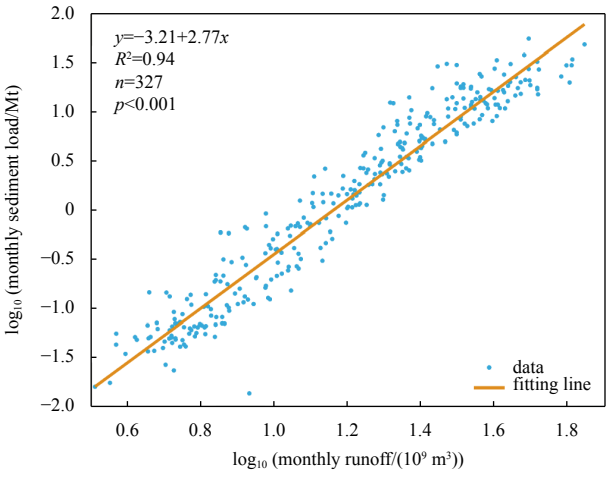

Fig. 9. Correlational relationship between logarithmic monthly runoff and logarithmic monthly sediment load.

We obtained sediment fluxes at Makou with and without the impact of upstream human activities. However, the sediment flux at Makou cannot represent the sediment load that eventually enters the ME. The sediment input to the ME could be obtained from the sediment flux at Makou by applying an appropriate ratio. According to Luo et al. (2007), the amount of sediment entering the ME was approximately 30.80% of that observed at the Gaoyao before 1991. In addition, by analyzing historical observation data, we found that the sediment quantity at Makou was 93.45% of that at Gaoyao. Thus, 32.96% of the sediment observed at Makou finally entered the ME.

If there were no human activities in the downstream reaches (i.e., the reaches between Makou and the ME), this ratio could also have been applied from 1992 to 2003. However, Luo et al. (2007) found that large-scale sand excavation occurred in downstream reaches during 1992–1999. Intense and unplanned sand excavation activities continued until the early 2000s, when authorities enacted regulations and policies to ban sand excavation. Therefore, the influence of human activities downstream of the Xijiang River on sediment transport in ME should be investigated.

It has been shown that human activities represented by sand excavation have significantly changed the morphology of the river channels between Makou and the ME, contributing to a shift from sedimentation to erosion (Han et al., 2010; Liu et al., 2011, 2018). The erosion of river channels may have brought more sediment into the downstream estuary than before. In addition, sand excavation and channel dredging may also cause resuspension of riverbed sediment, which may also lead to increased sediment input to the downstream estuary.

Using survey data from July 1999 to February 2001, we obtained the ratio between the sediment input to the ME and the sediment flux of Makou affected by downstream human activities during the wet and dry seasons (Tables 5 and 6). The results showed that human activities downstream (e.g., sand excavation and channel dredging) led to an increase in sediment concentration in the ME. Instead of reducing sediment input to the ME, human activities have increased it. Analysis of the seasonal distribution of the sediment load at Makou shows that the wet season accounts for 95% of the total sediment transport. Based on these

Table 5. Sediment fluxes at the main cross-sections of the Xijiang River during the survey in wet season

Station	Makou	Tianhe	Right Denglongshan	Left Denglongshan	Sed_{ME}/Sed_{Makou}
Net sediment output/t	5 118 768	2 269 100	1 149 800	1 161 500	45.15%
Mean sediment concentration/(kg·m^{-3})	0.304	0.295	0.378	0.392	–

Note: – means no data. ME: Modaomen Estuary.

Table 6. Sediment fluxes at the main cross-sections of the Xijiang River during the survey in dry season

Station	Makou	Tianhe	Right Denglongshan	Left Denglongshan	Sed_{ME}/Sed_{Makou}
Net sediment output/t	21 838	12 197	11 152	6 689.1	81.70%
Mean sediment concentration/(kg·m^{-3})	0.015	0.018	0.042	0.025	–

Note: – means no data. ME: Modaomen Estuary.

data, we estimated that the sediment input of ME was 46.98% of the sediment flux at Makou during 1992–2003 when downstream human activities occurred.

Subsequently, we estimated the sediment input to the ME based on sediment ratios for the two periods. The average annual sediment input to the ME was 26.08 Mt and 25.94 Mt for 1964–1983 and 1983–2003, respectively. Correspondingly, the average annual sediment load at Makou was 79.12 Mt and 64.64 Mt for these two periods. Without the influence of upstream human activities, the average annual sediment transport at Makou would be 74.25 Mt in 1983–2003. The sediment load at Makou was reduced by 13% because of upstream human activities. However, the sediment entering the ME was almost unchanged during the two periods because of human activities in the downstream reaches.

The morphological evolution of the ME causes more sediment to deposit in the estuary area. Based on the data of sediment input and the evolution of underwater topography, we calculated the sediment budget of the ME during 1964–1983 and 1983–2003 (Table 7). The net deposition of the consistent water area in each period was obtained from the analysis of underwater topography evolution. For areas that have changed from water to land, we estimated the volume from seabed to high tide as sediment accumulation. The dry bulk density of the sediment was then used to convert the sediment volume into sediment mass. For the value of dry bulk density, we referred to previous studies (Hillel, 2013; Wei et al., 2021). There was no significant difference in sediment input between the two periods, but the transformation of water areas into land during the period 1983–2003 increased the sediment capture ratio in the ME from 33.89% to 44.86%. In general, the morphological evolution of the ME promoted the effective utilization of sediment input.

Regarding sediment inputs of estuaries, many studies have often referred to long-term data observed at the stations that are not close to the estuary because of the absence of long-term sediment observation stations in estuaries. Our rough assessment suggests that this can sometimes lead to large deviations. More detailed studies should be carried out to investigate the true sediment inputs of estuaries.

4.2 *Impacts of human activities on shoreline evolution*

In the coastal zone, shoreline changes could be caused by various factors, including natural and anthropogenic factors, such as hurricane impact, sea-level change, variations in coastal circulation, riverine discharge change, gravel mining, and land reclamation (Cooper and Pilkey, 2004; Dean and Houston, 2016; Fearnley et al., 2009; Hansen et al., 2013; San-Nami et al., 2013; Zhu et al., 2016). Studies on the shoreline evolution in other estuaries revealed that changes in the amount of sediment input alter the evolutionary trend of the estuarine shoreline (Cui and Li, 2011; Besset et al., 2019). According to our calculations, the average annual sediment input of the ME during 1964–1983 and 1983–2003 is almost the same. Therefore, sediment input may not be the main influencing factor of shoreline evolution. For the long-term evolution of the shoreline, it is difficult to extract the contribution of individual impact factors from shoreline change, except for land reclamation. Using land reclamation data makes it easy to isolate the direct contribution of land reclamation from the results, whereas the indirect effects could not be identified easily.

We extracted the reclaimed shore area from the remote sensing images by using manual visual interpretation based on the basic characteristics of the land reclamation project. The land reclamation dataset was constructed with respect to the land reclamation project information in the ME from the literature (Han et al., 2010; Jia et al., 2013). We compared the land reclamation areas for each period in Fig. 10 with the historical shoreline data in Fig. 4, and most of the land reclamation projects and shoreline changes match well. To estimate the detailed contribution of land reclamation to shoreline evolution, we listed the relative statistics in Table 8.

In the first four periods, land reclamation contributed to more than 85% of the land increase in the study area. Especially during 1999–2003, the contribution was more than 98%; thus, land reclamation was a critical factor in shoreline change. Similar findings were found in other large estuaries or deltas. Chu et al. (2013) found that in the situation of sediment transport reduction due to the operation of the Three Gorges Dam, the shoreline of the Changjiang River Delta continued to advance seaward, and coastal engineering, especially sea reclamation works, played an important role. Yang et al. (2019) showed that reclamation reduced the water area of the Lingding Bay. van der Wal et al. (2002) analyzed bathymetric maps and remote sensing images and found that dike construction and land reclamation accelerated the siltation and intertidal area reduction in Ribble Estuary.

Considering that there are other unaccounted human activities, we determined that anthropogenic influence was the most prominent factor in shoreline evolution during the first four periods. However, the contribution of land reclamation decreased by 36% between 2003 and 2017. The land increase during this period was 0.71 km^2 but was over 20 km^2 in other periods. Moreover, the mean reclamation rate was 0.02 km^2/a, and it was more than 4.5 km^2/a in the former periods. As elaborated in Section 3.1, the shoreline remained relatively stable after 2003, which was probably due to the limitation of land reclamation activities.

These results demonstrate that shoreline change in the ME was strongly influenced by human activities during the four periods: 1973–1987, 1987–1991, 1991–1999, and 1999–2003. Land reclamation alone contributes to more than 85% of the shoreline change, and human activities are not accounted for. Undoubtedly, human activities dominated the evolution of the shoreline

Table 7. Sediment input, sedimentation, and escape of the Modaomen Estuary in different periods

Period	1964–1983	1983–2003
Averaged annual sediment input/(Mt·a^{-1})	26.08	25.94
Total sediment input (S_{total})/Mt	495.52	518.80
Net siltation amount within water area (V_w)/(10^6 m^3)	120.50	−3.78
Net sediment increases within water area (S_w=V_w×ρ_b)/Mt*	132.55	−4.16
Sediment volume of newly formed land areas (V_r)/(10^6 m^3)	32.17	215.36
Sediment mass of newly formed land areas (S_r=V_r×ρ_b)/Mt*	35.39	236.90
Total escaped sediment mass (S_e=S_{total}−S_w−S_r)/Mt	327.58	286.06
Capture ratio of sediment ((S_w+S_r)/S_{total}×100%)	33.89	44.86

Note: *The dry bulk density ρ_b used in the calculation is equal to 1.1 t/m^3.

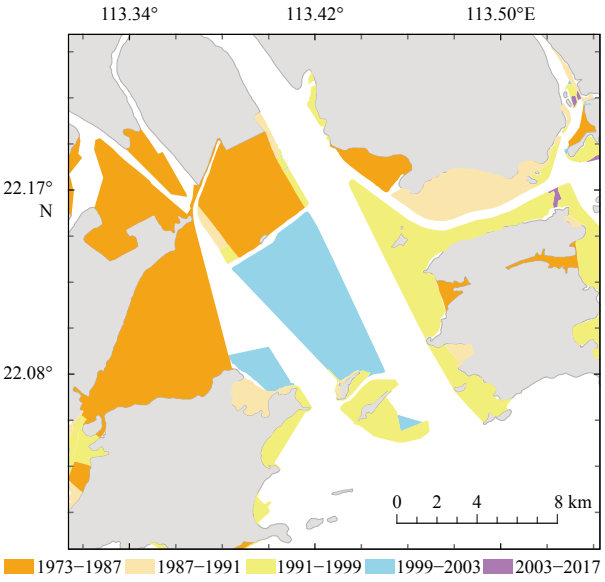

Fig. 10. Land reclamation projects for each period.

before 2003. After 2003, land reclamation was limited and may no longer have been the main cause of shoreline evolution.

4.3 *Impacts of human activities on subaqueous topography evolution*

Because the sedimentation process of estuaries is complex, making reasonable simplifications for the discussion of dominant factors is necessary. In the prior calculations, we obtained the variation in sediment input under the disturbance of upstream human activities. In addition, according to Wu et al. (2016b), a linear correlation is between the amount of sediment input and mean siltation rate for a natural local siltation environment. With this information, we can explore the shift in the siltation state under the influence of human activities. The siltation state is determined by the sediment input and mean siltation rate of the estuary. Thereafter, we could isolate the contribution of the types of human activities to siltation rate changes.

To evaluate the impact of human activities on the siltation rate, we first had to establish the relationship between the siltation rate and sediment in the natural state. The shoreline comparison in Fig. 5 shows that land reclamation during 1964–1983 was not drastic and had little impact on the sediment deposition environment of the estuary. In addition, a large amount of sand excavation in the Zhujiang River Delta started in the mid-1980s (Luo et al., 2007). Therefore, we could set the siltation rate of the ME from 1964 to 1983 as undisturbed by human activities. Using Wu's methodology, we assumed that a stable linear positive relationship was between the sediment input and siltation rate in the research area during 1964–1983.

Two siltation rate points are necessary for a linear relationship between sediment input and siltation rate. The siltation rate and annual sediment input during 1964–1983 provide one example. For the region outside the ME, Wu et al. (2016b) found that erosion and siltation reached a dynamic equilibrium (the siltation rate was zero) when the sediment input decreased to approximately 18.64 Mt/a. Because our research area is closer to the river channel than the study area, there should be a greater siltation capacity in our research area. Therefore, the annual sediment flux should be less than 18.64 Mt/a when the mean siltation rate is zero in the study area. In addition, in the most extreme situations, the area may reach a balance between erosion and siltation because no sediment is transported into the research region. Using the aforementioned information, we established two siltation state transition lines (Fig. 11), and the true transition line of our research area should be somewhere in between. When the local sedimentary environment is not disturbed by human activity, the siltation state moves along the line.

Based on the relationship between runoff and sediment transport in Fig. 9, the sediment transport of Makou in 1997–2003 without human disturbance was obtained. Subsequently, the mean sediment input of the ME from 1983 to 2003 was computed to reconstruct the siltation states (B1 and B2 in Fig. 11). States B1 and B2 represent natural siltation states without human impact. Because of upstream human interventions such as river damming and sand excavation, a large amount of sediment is lost. Consequently, the siltation state moves from B1 (or B2) to C1 (or C2) along the siltation transition line. During this process, the downstream river reaches and the local sedimentary environment in the ME remain stable. The ratio between the sediments of Makou and ME was unchanged. Therefore, the change in the deposition rate was completely controlled by the variation in the sediment budget at Makou (i.e., upstream human activities).

Human activities in the downstream channel increased the sediment entering the ME, with the increase outweighing the decrease in sediment due to upstream human activities. This process is expressed as a transition from C1 (or C2) to D1 (or D2) (Fig. 11). The transition from state D1 (or D2) to state E represents the impact of local human activities on the local sedimentary environment, resulting in a variation in the siltation rate from 15.34 mm/a (or 15.19 mm/a) to –1.02 mm/a. Local human activities conducted in the estuary include channel deepening, sand dredging, land reclamation, and guide dike construction. Consequently, the transition from state B1 (or B2) to state E represents the combined effect of upstream, downstream, and local human activity.

By checking the variation in the mean siltation rate in different siltation states, we quantified the contribution of different human activities to the change in the siltation rate. The mean siltation rate represents the overall evolution of subaqueous topography. The contribution of upstream human activities was between 12% and 40%, that of downstream human activities was between –18% and –58%, and that of local human activities was between 106% and 60%. Negative values imply that downstream human activities contributed to an increase rather than a decrease in the mean siltation rate.

Although the anthropogenic forces in the upper Xijiang River directly reduced the riverine sediment load by 13%, this factor

Table 8. Statistics of land area increase and reclamation in each period

Period	1973–1987	1987–1991	1991–1999	1999–2003	2003–2017
Land increase (LI)/km^2	83.12	21.32	44.74	31.36	0.71
Reclaimed area (RA)/km^2	79.39	18.14	38.99	30.78	0.26
Percentage of reclaimed area (RA/LI)/%	95.51	85.08	87.15	98.15	36.50
Mean reclamation rate (RA/length of the period)/(km^2·a^{-1})	5.67	4.53	4.87	7.69	0.02

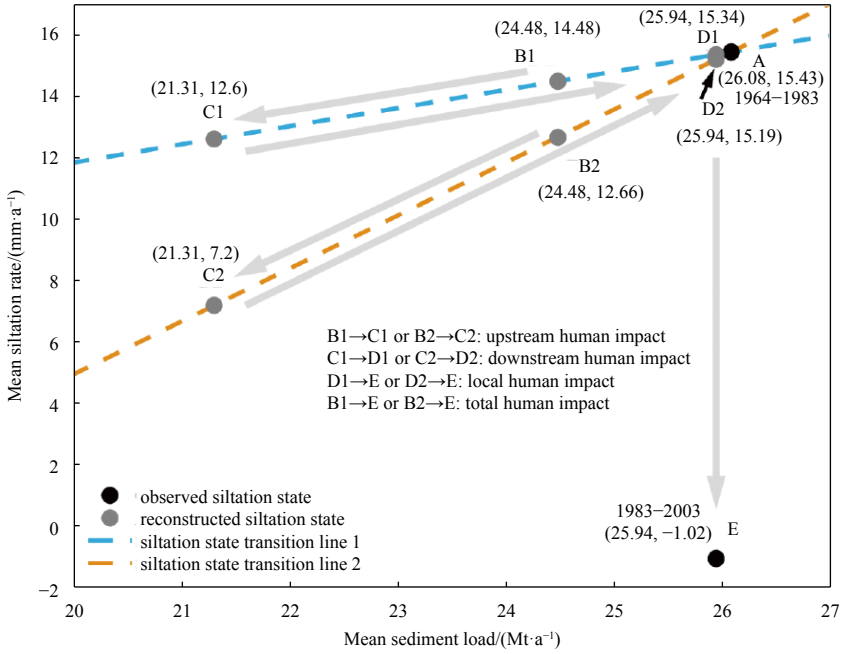

Fig. 11. Siltation state shift under the human impact. Siltation state transition line 1 passes points (0, 0) and (26.08, 15.43); siltation state transition line 2 goes through (17.14, 0) and (26.08, 15.43). States B1 and B2 denote siltation states with no human impact. States C1 and C2 represent siltation states only with upstream human activities. States D1 and D2 mean siltation states affected by upstream and downstream human activities. State E represents the siltation state under the influence of upstream, downstream, and local human activities.

was not critical for the significant change in the siltation rate of the ME during 1983–2003. Remarkably, human activities, such as sand excavation in the downstream river channel can increase sediment input to the ME. The increment exceeded the sediment reduction due to the dam construction in the upstream reaches. Furthermore, Fig. 11 shows that local human activities have absolute dominance over the evolution of the subaqueous topography. Under the influence of local human activities, the evolution of the underwater topography of the ME has changed significantly from siltation to slight erosion.

The contribution of local human activities we obtained represents the total impact of all human activities occurring in the ME during 1983–2003, rather than referring to a particular anthropogenic intervention project or a particular type of human activity. Human activities occurring in estuaries are varied, and their effects on the underwater topography of estuaries are also different. Land reclamation projects reduce the area of water in estuaries and narrow runoff transport channels so that sediment can be transported further away from outlets (Wei et al., 2021). Sand excavation and channel dredging can cause erosion of estuary subaqueous deltas and increase the average depth of estuaries. (Wu et al., 2016a, 2016b). In addition, we note that different estuaries may respond differently to the variations of sediment input, and that the mechanisms of morphological evolution are not consistent across estuaries. For instance, Dai et al. (2014) found that the evolution of the Changjiang River submerged delta appears to be poorly related to upstream sand transport. Despite the huge sediment load trapped by the Three Gorges Dam, the Changjiang River submerged delta did not experience eroding as expected. Extreme floods and storm surges have a greater impact on the evolution of the Changjiang River subaqueous delta than upstream sediment changes.

Our discussion has been based on acceptable simplifying assumptions; however, the results have essential implications for river and estuary management. A more comprehensive study than ours would be worthwhile if more data would become available.

5 Conclusions

We conducted a systematic study on the evolution of MEs in recent decades, covering variations in shoreline and subaqueous topography. In addition, we quantified the contribution of human activities to morphological evolution.

From 1973 to 2003, the shoreline of the ME underwent dramatic changes: approximately 49% of the water area turned to land. Shoreline changes significantly altered the hydrodynamic environment, with shoals disappearing in patches and river channel narrowing. In this process, land reclamation projects dominated the shoreline evolution, with a direct impact of more than 85%. After 2003, the shoreline remained relatively stable, probably due to limited land reclamation, and shoreline evolution was dominated by natural processes.

The evolution of subaqueous topography was slightly disturbed by human activities in 1964–1983. Shallowing was the main process in this period, except in some areas of the main channel. With an average sediment flux of 26.08 Mt/a, the average siltation rate was 15.43 mm/a. From 1983 to 2003, DEM analysis revealed that shallow shoals were increasingly shallowed and finally disappeared, whereas the mid-depth area increased. In addition, the estuary changed from sedimentation to slight erosion, with a mean siltation rate of –1.02 mm/a. Based on the runoff–sediment relationship, the sediment load observed at Makou decreased by 13% under the disturbances of human activities upstream during this period. By contrast, sand excavation in downstream reaches of the river significantly increases the amount of sediment entering the ME. Subsequently, referring to the siltation state transition relationship, our estimates show that although upstream and downstream human activities may have

contributed significantly, local human activities are the dominant force in the evolution of underwater topography in the estuarine region.

Our findings suggest that local human activities are critical to the evolution of estuarine morphology and should receive increased attention in the management of ME. The findings of this study also have reference significance for other estuaries.

References

Acciarri A, Bisci C, Cantalamessa G, et al. 2016. Anthropogenic influence on recent evolution of shorelines between the Conero Mt. and the Tronto R. mouth (southern Marche, Central Italy). CATENA, 147: 545–555, doi: 10.1016/j.catena.2016.08.018

Besset M, Anthony E J, Bouchette F. 2019. Multi-decadal variations in delta shorelines and their relationship to river sediment supply: an assessment and review. Earth-Science Reviews, 193: 199–219, doi: 10.1016/j.earscirev.2019.04.018

Chen Xiaowen, Liu Xia, Zhang Wei. 2011. Shore reclamation in Zhujiang River Esturay and its impact analysis. Journal of Hohai University (Natural Sciences) (in Chinese), 39(1): 39–43

Chu Zhongxin, Yang Xuhui, Feng Xiuli, et al. 2013. Temporal and spatial changes in coastline movement of the Yangtze Delta during 1974–2010. Journal of Asian Earth Sciences, 66: 166–174, doi: 10.1016/j.jseaes.2013.01.002

Cooper J A G, Pilkey O H. 2004. Sea-level rise and shoreline retreat: time to abandon the Bruun Rule. Global and Planetary Change, 43(3–4): 157–171

Cowart L, Walsh J P, Corbett D R. 2010. Analyzing estuarine shoreline change: a case study of cedar Island, North Carolina. Journal of Coastal Research, 26(5): 817–830

Cui Buli, Li Xiaoyan. 2011. Coastline change of the Yellow River Estuary and its response to the sediment and runoff (1976–2005). Geomorphology, 127(1–2): 32–40

Cunliffe A M, Tanski G, Radosavljevic B, et al. 2019. Rapid retreat of permafrost coastline observed with aerial drone photogrammetry. The Cryosphere, 13(5): 1513–1528, doi: 10.5194/tc-13-1513-2019

Dai Zhijun. 2021. Changjiang Riverine and Estuarine Hydro-morphodynamic Processes: in the Context of Anthropocene Era. Singapore: Springer

Dai Zhijun, Liu J T. 2013. Impacts of large dams on downstream fluvial sedimentation: an example of the Three Gorges Dam (TGD) on the Changjiang (Yangtze River). Journal of Hydrology, 480: 10–18, doi: 10.1016/j.jhydrol.2012.12.003

Dai Zhijun, Liu J T, Wei Wen, et al. 2014. Detection of the Three Gorges Dam influence on the Changjiang (Yangtze River) submerged delta. Scientific Reports, 4: 6600, doi: 10.1038/srep06600

Dai Shibao, Lu Xixi. 2014. Sediment load change in the Yangtze River (Changjiang): a review. Geomorphology, 215: 60–73, doi: 10.1016/j.geomorph.2013.05.027

Dai Zhijun, Mei Xuefei, Darby S E, et al. 2018. Fluvial sediment transfer in the Changjiang (Yangtze) river-estuary depositional system. Journal of Hydrology, 566: 719–734, doi: 10.1016/j.jhydrol.2018.09.019

Dai Shibao, Yang Shilun, Cai Aimin. 2008. Impacts of dams on the sediment flux of the Zhujiang River, southern China. CATENA, 76(1): 36–43, doi: 10.1016/j.catena.2008.08.004

Day J W, Giosan L. 2008. Survive or subside?. Nature Geoscience, 1(3): 156–157

Dean R G, Houston J R. 2016. Determining shoreline response to sea level rise. Coastal Engineering, 114: 1–8, doi: 10.1016/j.coastaleng.2016.03.009

Fanos A M. 1995. The impact of human activities on the erosion and accretion of the Nile Delta coast. Journal of Coastal Research, 11(3): 821–833

Fearnley S M, Miner M D, Kulp M, et al. 2009. Hurricane impact and recovery shoreline change analysis of the Chandeleur Islands, Louisiana, USA: 1855 to 2005. Geo-Marine Letters, 29(6): 455–466, doi: 10.1007/s00367-009-0155-5

Ford M. 2013. Shoreline changes interpreted from multi-temporal aerial photographs and high resolution satellite images: Wotje Atoll, Marshall Islands. Remote Sensing of Environment, 135: 130–140, doi: 10.1016/j.rse.2013.03.027

Frihy O E, Debes E A, El Sayed W R. 2003. Processes reshaping the Nile delta promontories of Egypt: pre- and post-protection. Geomorphology, 53(3–4): 263–279

Gellis A C, Noe G B. 2013. Sediment source analysis in the Linganore Creek watershed, Maryland, USA, using the sediment fingerprinting approach: 2008 to 2010. Journal of Soils and Sediments, 13(10): 1735–1753, doi: 10.1007/s11368-013-0771-6

Gong Wenping, Shen Jian. 2011. The response of salt intrusion to changes in river discharge and tidal mixing during the dry season in the Modaomen Estuary, China. Continental Shelf Research, 31(7–8): 769–788

Grill G, Lehner B, Thieme M, et al. 2019. Mapping the world's free-flowing rivers. Nature, 569(7755): 215–221, doi: 10.1038/s41586-019-1111-9

Han Zhiyuan, Tian Xiangping, Ou Suying. 2010. Impacts of Large-scale human activities on riverbed morphology and tidal dynamics at modaomen estuary. Scientia Geographica Sinica (in Chinese), 30(4): 582–587

Hansen J E, Elias E, List J H, et al. 2013. Tidally influenced alongshore circulation at an inlet-adjacent shoreline. Continental Shelf Research, 56: 26–38, doi: 10.1016/j.csr.2013.01.017

Healy M G, Hickey K R. 2002. Historic land reclamation in the intertidal wetlands of the Shannon Estuary, western Ireland. Journal of Coastal Research, 36(10036): 365–373

Hillel D. 2013. Introduction to Soil Physics. New York: Academic Press

Himmelstoss E A, Henderson R E, Kratzmann M G, et al. 2018. Digital shoreline analysis system (DSAS) version 5.0 user guide. Reston: U. S. Geological Survey

Jia Liangwen, Pan Shunqi, Wu Chaoyu. 2013. Effects of the anthropogenic activities on the morphological evolution of the Modaomen Estuary, Zhujiang River Delta, China. China Ocean Engineering, 27(6): 795–808, doi: 10.1007/s13344-013-0065-1

Jones B M, Grosse G, Arp C D, et al. 2011. Modern thermokarst lake dynamics in the continuous permafrost zone, northern Seward Peninsula, Alaska. Journal of Geophysical Research: Biogeosciences, 116(G2): G00M03

Kong Dongxian, Miao Chiyuan, Borthwick A G L, et al. 2015. Evolution of the Yellow River Delta and its relationship with runoff and sediment load from 1983 to 2011. Journal of Hydrology, 520: 157–167, doi: 10.1016/j.jhydrol.2014.09.038

Lehner B, Liermann C R, Revenga C, et al. 2011. High-resolution mapping of the world's reservoirs and dams for sustainable river-flow management. Frontiers in Ecology and the Environment, 9(9): 494–502, doi: 10.1890/100125

Liu Feng, Hu Shuai, Guo Xiaojuan, et al. 2018. Recent changes in the sediment regime of the Zhujiang River (South China): causes and implications for the Zhujiang River Delta. Hydrological Processes, 32(12): 1771–1785, doi: 10.1002/hyp.11513

Liu Feng, Tian Xiangping, Han Zhiyuan, et al. 2011. Analysis of river channel evolution of Modaomen channel of Xijiang River in past forty years. Journal of Sediment Research (in Chinese), (1): 45–50

Liu Feng, Yuan Lirong, Yang Qingshu, et al. 2014. Hydrological responses to the combined influence of diverse human activities in the Zhujiang River Delta, China. CATENA, 113: 41–55, doi: 10.1016/j.catena.2013.09.003

Loveland T R, Dwyer J L. 2012. Landsat: building a strong future. Remote Sensing of Environment, 122: 22–29, doi: 10.1016/j.rse.2011.09.022

Luo Xiangxin, Yang Shilun, Zhang Jing. 2012. The impact of the Three Gorges Dam on the downstream distribution and texture of sediments along the middle and lower Yangtze River (Changjiang) and its estuary, and subsequent sediment dispersal in the East China Sea. Geomorphology, 179: 126–140, doi: 10.1016/j.geomorph.2012.05.034

Luo Xianlin, Zeng E Y, Ji Rongyao, et al. 2007. Effects of in-channel

sand excavation on the hydrology of the Zhujiang River Delta, China. Journal of Hydrology, 343(3–4): 230–239

Matin N, Hasan G M J. 2021. A quantitative analysis of shoreline changes along the coast of Bangladesh using remote sensing and GIS techniques. CATENA, 201: 105185, doi: 10.1016/j.catena.2021.105185

McFeeters S K. 1996. The use of the Normalized Difference Water Index (NDWI) in the delineation of open water features. International Journal of Remote Sensing, 17(7): 1425–1432, doi: 10.1080/01431169608948714

Meade R H. 1982. Sources, sinks, and storage of river sediment in the Atlantic drainage of the United States. The Journal of Geology, 90(3): 235–252, doi: 10.1086/628677

Mei Xuefei, Dai Zhijun, Du Jinzhou, et al. 2015. Linkage between Three Gorges Dam impacts and the dramatic recessions in China's largest freshwater lake, Poyang Lake. Scientific Reports, 5: 18197, doi: 10.1038/srep18197

Nilsson C, Reidy C A, Dynesius M, et al. 2005. Fragmentation and flow regulation of the world's large river systems. Science, 308(5720): 405–408, doi: 10.1126/science.1107887

Pritchard D W. 1967. What is an estuary: physical viewpoint. American Association for the Advancement of Science, 83: 3–5

Roccati A, Faccini F, Luino F, et al. 2019. Morphological changes and human impact in the Entella River floodplain (Northern Italy) from the 17th century. CATENA, 182: 104122, doi: 10.1016/j.catena.2019.104122

San-Nami T, Uda T, Onaka S. 2013. Long-term shoreline recession on eastern Bali Coast caused by riverbed mining. In: Proceedings of the 7th International Conference on Asian and Pacific Coasts. Bali: Hasanuddin University, 275–282

Stanley D J, Warne A G. 1993. Nile delta: recent geological evolution and human impact. Science, 260(5108): 628–634, doi: 10.1126/science.260.5108.628

Thieler E R, Himmelstoss E A, Zichichi J L, et al. 2009. The digital shoreline analysis system (DSAS) version 4.0-An ArcGIS extension for calculating shoreline change. Reston: U. S. Geological Survey

van der Wal D, Pye K, Neal A. 2002. Long-term morphological change in the Ribble Estuary, northwest England. Marine Geology, 189(3–4): 249–266

Wang Jie, Dai Zhijun, Mei Xuefei, et al. 2020. Tropical cyclones significantly alleviate mega—deltaic erosion induced by high riverine flow. Geophysical Research Letters, 47(19): e2020GL089065

Wei Xing, Cai Shuqun, Zhan Weikang. 2021. Impact of anthropogenic activities on morphological and deposition flux changes in the Zhujiang River Estuary, China. Scientific Reports, 11(1): 16643, doi: 10.1038/s41598-021-96183-0

Wu Ziyin, Milliman J D, Zhao Dineng, et al. 2018. Geomorphologic changes in the lower Zhujiang River Delta, 1850–2015, largely due to human activity. Geomorphology, 314: 42–54, doi: 10.1016/j.geomorph.2018.05.001

Wu Ziyin, Saito Y, Zhao Dineng, et al. 2016a. Impact of human activities on subaqueous topographic change in Lingding Bay of the Zhujiang River Estuary, China, during 1955–2013. Scientific Reports, 6: 37742, doi: 10.1038/srep37742

Wu Chuangshou, Yang Shilun, Huang Shichang, et al. 2016b. Delta changes in the Zhujiang River Estuary and its response to human activities (1954–2008). Quaternary International, 392: 147–154, doi: 10.1016/j.quaint.2015.04.009

Yang Shilun, Belkin I M, Belkina A I, et al. 2003. Delta response to decline in sediment supply from the Yangtze River: evidence of the recent four decades and expectations for the next half-century. Estuarine, Coastal and Shelf Science, 57(4): 689–699

Yang Liuzhu, Liu Feng, Gong Wenping, et al. 2019. Morphological response of Lingding Bay in the Zhujiang River Estuary to human intervention in recent decades. Ocean & Coastal Management, 176: 1–10

Yang Shilun, Milliman J D, Li Peng, et al. 2011. 50, 000 dams later: erosion of the Yangtze River and its delta. Global and Planetary Change, 75(1–2): 14–20

Yang Zuosheng, Wang Houjie, Saito Y, et al. 2006. Dam impacts on the Changjiang (Yangtze) River sediment discharge to the sea: the past 55 years and after the Three Gorges Dam. Water Resources Research, 42(4): W04407

Yang Shilun, Zhang Jianbo, Xu Xiaojun. 2007. Influence of the Three Gorges Dam on downstream delivery of sediment and its environmental implications, Yangtze River. Geophysical Research Letters, 34(10): L10401, doi: 10.1029/2007GL029472

Zhang Shurong, Lu Xixi. 2009. Hydrological responses to precipitation variation and diverse human activities in a mountainous tributary of the lower Xijiang, China. CATENA, 77(2): 130–142, doi: 10.1016/j.catena.2008.09.001

Zhang Qiang, Xu Chongyu, Chen Yongqin David, et al. 2009. Abrupt behaviors of the streamflow of the Zhujiang River basin and implications for hydrological alterations across the Zhujiang River Delta, China. Journal of Hydrology, 377(3–4): 274–283

Zhang Wei, Xu Yang, Hoitink A J F, et al. 2015. Morphological change in the Zhujiang River Delta, China. Marine Geology, 363: 202–219, doi: 10.1016/j.margeo.2015.02.012

Zhu Meisha, Sun Tao, Shao Dongdong. 2016. Impact of land reclamation on the evolution of shoreline change and nearshore vegetation distribution in Yangtze River Estuary. Wetlands, 36(S1): 11–17, doi: 10.1007/s13157-014-0610-6